Proceedings Paper:
Penava, D, Anić, F, Sarhosis, V orcid.org/0000-0002-8604-8659 et al. (1 more author) (2019) Distribution of Shear Resistance Among Components of R. C. Frames with Masonry Infill Walls Containing Confined Door and Window Openings. In: Papadrakakis, M and Fragiadakis, M, (eds.) Proceedings of the 7th International Conference on Computational Methods in Structural Dynamics and Earthquake Engineering. COMPDYN 2019: 7th International Conference on Computational Methods in Structural Dynamics and Earthquake Engineering, 24 Jul - 26 Jun 2019, Crete, Greece. Eccomas Proceedia , pp. 2418-2430. ISBN 978-618-82844-6-3

https://doi.org/10.7712/120119.7084.18488

COMPDYN 2019
7th ECCOMAS Thematic Conference on
Computational Methods in Structural Dynamics and Earthquake Engineering
M. Papadrakakis, M. Fragiadakis (eds.)
Crete, Greece, 24–26 June 2019

DISTRIBUTION OF SHEAR RESISTANCE AMONG COMPONENTS OF R. C. FRAMES WITH MASONRY INFILL WALLS CONTAINING CONFINED DOOR AND WINDOW OPENINGS

Davorin Penava[1], Filip Anić[1], Vasilis Sarhosis[2], and Lars Abrahamczyk[3]

[1] Josip Juraj Strossmayer University of Osijek, Faculty of Civil Engineering and Architecture Osijek, 3 Vladimir Prelog Str., 31000 Osijek, Croatia
{davorin.penava,filip.anic}@gfos.hr

[2] Newcastle University, School of Engineering, Newcastle upon Tyne, NE1 7RU, United Kingdom
vasilis.sarhosis@newcastle.ac.uk

[3] Bauhaus-University Weimar, Earthquake Damage Analysis Centre (EDAC), Marienstraße 13B, 99423 Weimar, Germany
lars.abrahamczyk@uni-weimar.de

Abstract

In earthquake resistant design of r. c. frame structures with unreinforced masonry infill walls, containing different in size and position window and door openings, confining elements (tie-columns) are crucial component of seismic detailing of the structure. Having construction of the masonry infill wall without confining elements along opening edges, seismic response prediction becomes unreliable, due to uncontrolled sequenced failure mode of masonry infill walls, its out-of-plane instability, unfavorable crack distribution and premature and total dis-integration. Confining elements are not subdued to design as moment-resisting r. c. frames and their construction details are based on simple recommendations. The aim of this study is, by usage of calibrated computational micromodel in computer program ATENA 2D Eng, to determine the shear resistance distribution among components of r. c. frames with masonry infill walls, containing confined door and window openings, at damage grades in compliance with EMS-98 scale.

Keywords: R. C. Frame, Unreinforced Masonry Infill Walls, Door and Window Opening, R. C. Confining Elements, Partial Shear Resistance.

1 INTRODUCTION

In earthquake resistant design of r. c. frame structures with unreinforced masonry infill walls, containing different in size and position window and door openings, confining elements (tie-columns) constitute an essential part of seismic detailing of the structure [1–3]. Construction of vertical r. c. confining elements along opening edges can significantly improve the seismic performance of the structure [4, 5]. On the other hand, having construction of the masonry infill wall without confining elements along opening edges, seismic response prediction becomes unreliable due to sequenced failure of masonry infill wall, out-of-plane instability, unfavorable crack distribution and premature and total collapse [6–13]. Confining elements are not subdued to design as moment-resisting r. c. frames and their construction details are based on simple recommendations.

The basis for this study were tested 1/2.5 scaled physical models of r. c. frames with masonry infill walls, containing centrically or eccentrically positioned medium size windows and door openings (opening to masonry infill wall area ratio A_o / A_i $\leqslant$ 15 % [14]), and walls without openings (see Figures 1 to 3 and Table 1), designed and constructed in compliance with [1–3] provisions, as moment-resisting frames by considering the medium ductility form of seismic construction detailing [4, 5]. Masonry infill walls were made of clay block masonry units that belonged to Group 2 and general purpose masonry mortar of M5 class which satisfied the seismic design requirements for unreinforced structural masonry walls. Model structures were divided in three groups (see Table 1), namely I, II and III. Group I models were same as models of Group II but without confining elements. Tests under cyclic in-plane shear action revealed the attaining of a very heavy damage of a masonry infill wall (DG 4 i.e. damage grade 4 in compliance with EMS-98 scale [15, 16]) at a drift ratio of about 1.25 %, compared to 0.5 % in a case without confining elements. Furthermore, confining elements contend the influence of opening and enabled the resistance of structure to horizontal seismic shear force equal as in the case without opening.

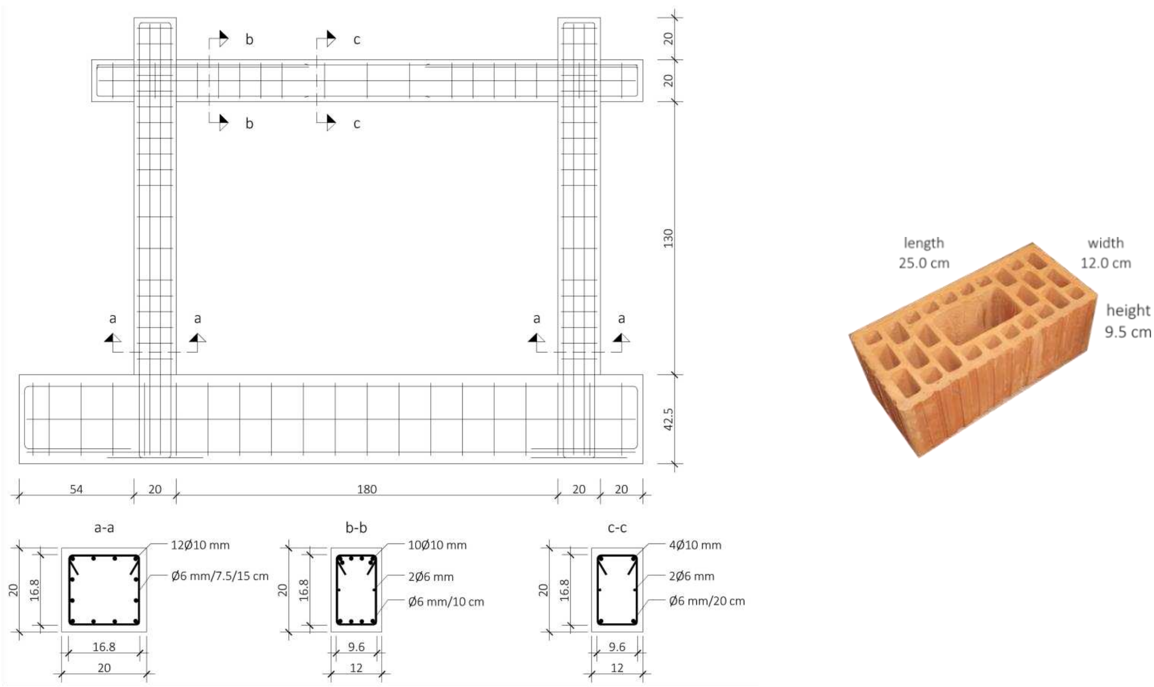

Figure 1: Design and construction detailing drawings of 1/2.5 scaled r. c. frame structure used in laboratory tests (left) and clay block masonry units used (right) [4,5]

Figure 2: Tested 1/2.5 scaled r. c. frame structures with masonry infill walls containing confined openings and walls without openings [4,5]

Specimen		Appearance of the specimen	Opening		Description
Group	**Mark**		**Type, area and area ratio**	**Position**	
II	1	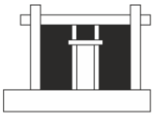	Door l_o/h_o=0.35/0.90 m A_o/A_i=0.14; =0.32 m^2	Centric e_o= l_i/2 =0.90 m	Specimens with confinement
	2	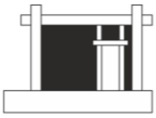	Window l_o/h_o=0.50/0.60 m A_o/A_i=0.13; A_o=0.30 m^2	Centric e_o= l_i/2 =0.90 m P=0.40 m	
	3	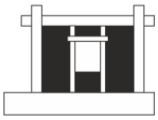	Door l_o/h_o=0.35/0.90 m A_o/A_i=0.14; A_o=0.32 m^2	Eccentric e_o=h_i/5+l_o/2=0.44 m	
	4	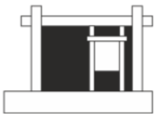	Window l_o/h_o=0.50/0.60 m A_o/A_i=0.13; A_o=0.30 m^2	Eccentric e_o=h_i/5+l_o/2=0.44 m P=0.40 m	
III	1	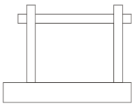	-	-	Reference specimens
	2	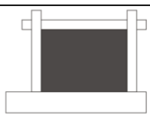	-	-	

Notations: A_o is the area of an opening and is equal to the height of the opening (h_o) multiplied by the length of the opening (l_o); A_i is the area of the masonry infill wall and is equal to the height of the masonry infill wall (h_i) multiplied by the length of the masonry infill wall (l_i); h_i is equal to 1.3 m; l_i is equal to 1.8 m; e_o is the eccentricity of the opening; t_i is the masonry infill wall thickness and is equal to 0.12 m; P is the parapet wall height.

Table 1: Classification and description of the specimens tested in the laboratory [4,5]

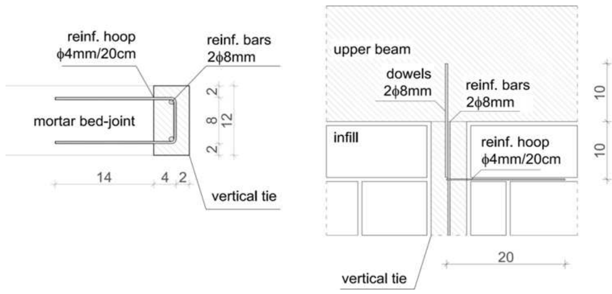

Figure 3: Vertical r. c. confining element reinforcement and construction details in the cross-section (left) and in elevation (right) [4,5]

At heavy damage of masonry infill wall (DG 3), occurring at drift ratio of 0.75 to 1 %, the confining elements along opening edge were vulnerable to shear failure in the vicinity of opening corners (see Figures 2 and 3).

The aim of this study is to determine the shear resistance distribution among components of tested r. c. frames with masonry infill walls, containing confined door and window openings, and walls without openings, at damage grades in compliance with EMS-98 scale [15,16] by using computational micromodels and by employing the nonlinear static analysis.

A particular attention was given to the shear resistance contribution and design of vertical r. c. confining elements constructed along opening edges.

2 COMPUTATIONAL MICROMODEL

A 2D computational simplified micromodel was developed in computer program ATENA 2D Eng [17–19] and calibrated against previously described 1/2.5 scaled tested physical models [4,5], as described in detail in [20] (see Figure 4).

The adopted modelling approach, compared to other available modelling solutions e.g. [21–27], had the ability to fully simulate tests, to take into account opening type, size and position and confining elements in a straight forward manner, to simulate the complex failure mechanism precisely and to distinguish the shear resistance distribution among the structural members [20,28–33].

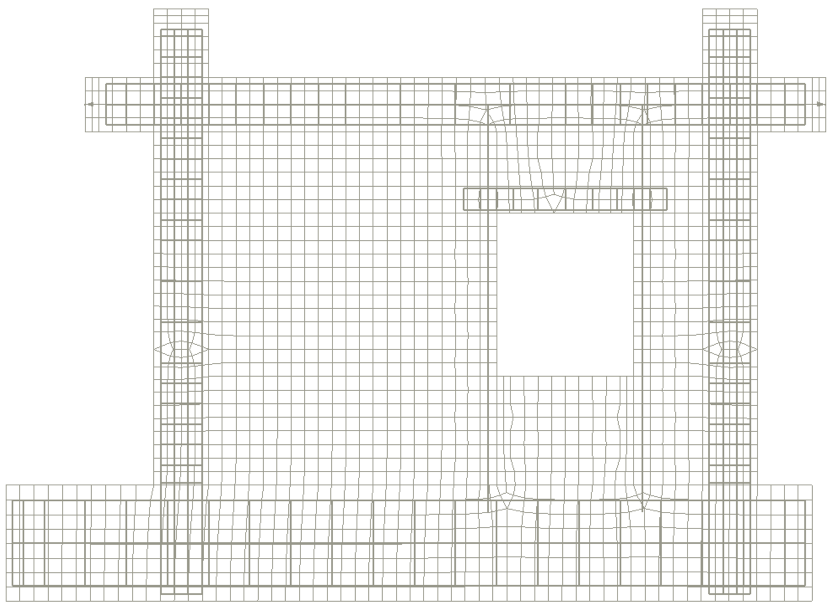

Figure 4: Computational micromodel of r. c. frame with masonry infill wall built in ATENA 2D Eng [19]

The model was limited to 2D actions, as it was in the tests. The geometry characteristics of the model were adopted the same as of the tested 1/2.5 scale physical models (see Figures 1 to 4). The model was built by using iso-parametric plane FEs (9-node quadrilateral and 6-node triangular) for concrete and masonry units, and truss elements (3-nodes) for reinforcement and gap elements for the interface. The finite element mesh size, based on convergence tests, corresponded to one quarter of the structural element size as shown in Figure 4.

The masonry units and masonry mortar interface (zero thickness interface) were modelled separately. The normal and tangential stiffness of the interface were estimated based on the expressions K_{nn}=E/t and K_{tt}=G/t respectively, where E and G are the modulus of elasticity and the shear modulus of the masonry unit, and t is the thickness of the mortar joint [17,18].

The adopted constitutiv laws for each individual material and its properties are given in Tables 2 to 6. Additionally, the special effect of masonry unit and masonry mortar joint interlocking was considered for the bed joints [34] by inclusion of the cohesion hardening–softening function (see Figure 5). All the material properties were determined by standard tests or by theoretical expressions.

Description	**Symbol**	**Value**	**Units**
Elastic modulus*	E	41000	MPa
Poisson's ratio	μ	0.2	-
Tensile strength	f_t	4	MPa
Compressive strength*	f_c	-58	MPa
Specific fracture energy	G_f	$1.20\cdot10^{-4}$	MN/m
Critical compressive displacement	w_d	$-1.0\cdot10^{-3}$	m
Eccentricity, defining the shape of the failure surface	E_{xc}	0.52	-
Multiplier for the direction of the plastic flow	β	0	-
Crack model coefficient (1.0 for Fixed, 0.0 for Rotated)	-	0	-
Plastic strain at compressive strength	ε_{CP}	$-1.417\cdot10^{-3}$	-
Reduction of compressive strength due to cracks	$f_{c,LIM}$	0.1	-
Crack shear stiffness factor	s_F	20	-
Aggregate size*	-	0.016	m
Crack spacing	s_{max}	0.125	m
Tension stiffening	c_{ts}	0.4	-
Note: *designates experimentally obtained value as described in [4,5]			

Table 2: Concrete properties for material model NonLinCementitious2

Description	**Symbol**	**Value**	**Units**
Elastic modulus*	E	210000	MPa
Yield strength*	σ_y	550	MPa
Ultimate strength*	σ_t	650	MPa
Strain at ultimate strength*	ε_{lim}	0.01	-
Bauschinger effect exponent	R	20	-
Menegotto–Pinto model parameter	C1	0.925	-
Menegotto–Pinto model parameter	C2	0.15	-
Note: *designates experimentally obtained value as described in [4,5]			

Table 3: Reinforcement properties for cycling reinforcement

Description	**Symbol**	**Value**	**Units**

Elastic modulus parallel to the head joints*	E_{hj}	5650	MPa
Elastic modulus parallel to the bed joints*	E_{bj}	850	MPa
Poisson's ratio	μ	0.1	-
Tensile strength*	f_t	1.8	MPa
Compressive strength parallel to the head joints*	f_c	-17.5	MPa
Compressive strength parallel to the bed joints*	f_c	-2.8	MPa
Type of tension softening	Exponential		
Specific fracture energy	G_f	$0.45 \cdot 10^{-4}$	MN/m
Crack model	Rotated		
Compressive strain at compressive strength in the uniaxial compressive test*	ε_C	$-1.358 \cdot 10^{-3}$	-
Reduction of compressive strength due to cracks	-	0.8	-
Type of compression softening	Crush Band		
Critical compressive displacement	w_d	$-5.0 \cdot 10^{-4}$	m
Shear retention factor	Variable		
Tension–compression interaction	Linear		
Note: *designates experimentally obtained value as described in [4,5]			

Table 4: Properties of the clay block masonry unit for model SBeta

Description	**Symbol**	**Value**	**Units**
Normal stiffness	K_{nn}	$5.65 \cdot 10^{5}$	MN/m^3
Tangential stiffness	K_{tt}	$2.57 \cdot 10^{5}$	MN/m^3
Cohesion*	c	0.35	MPa
Tensile strength*	f_t	0.2	MPa
Friction coefficient*	-	0.24	-
Minimum normal stiffness	$K_{nn,min}$	$5.65 \cdot 10^{2}$	MN/m^3
Minimum tangential stiffness	K_{ttmin}	$2.57 \cdot 10^{2}$	MN/m^3
Function tension softening–hardening	Not used		
Function cohesion softening–hardening	Used		
Note: *designates experimentally obtained value as described in [4,5]			

Table 5: Initial properties of bed joints

Description	**Symbol**	**Value**	**Units**
Normal stiffness	K_{nn}	$8.50 \cdot 10^{4}$	MN/m^3
Tangential stiffness	K_{tt}	$3.86 \cdot 10^{4}$	MN/m^3
Cohesion*			
Tensile strength*	Adopted from the bed joints		
Friction coefficient*			
Minimum normal stiffness	$K_{nn,min}$	$8.50 \cdot 10^{1}$	MN/m^3
Minimum tangential stiffness	K_{ttmin}	$3.86 \cdot 10^{1}$	MN/m^3
Note: *designates experimentally obtained value as described in [4,5]			

Table 6: Initial properties of head joints

The concrete of the confining elements and the lintel were represented by NonLinCementitious2concrete constitutive law. Its compressive strength was equal to 30 MPa, and other parameters were evaluated by theoretical expressions given in [17,18].

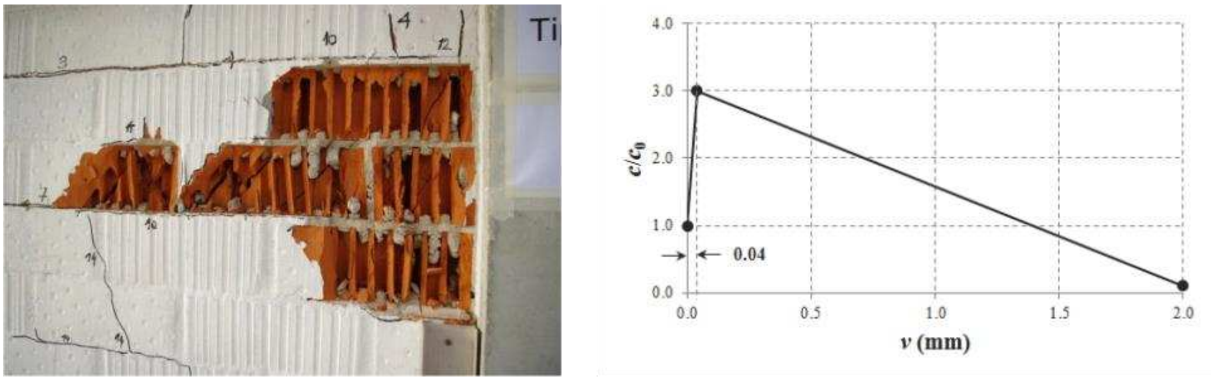

Figure 5: Mortar interlocking with the masonry units (left) and cohesion hardening–softening function (right)

3 ANALYSIS AND RESULTS

In order to determine the shear resistance among structure components, namely r. c. frame $V_{R,if,f}$ (kN), masonry infill wall $V_{R,if,i}$ (kN) and r. c. confining element $V_{R,if,c}$ (kN), a displacement controlled nonlinear static (pushover) analysis was employed up to the displacement d=28 mm i. e. drift ratio d_r=2 %. A d_r=2 % was adopted as the point of very heavy structural damage and destruction of the r. c. frame. The displacement controlled approach adopted, enabled observation of structure up to the drift ratio of 2 % (1.25 % was maximal drift in force controlled approach in tests) and of the shear resistance after maximum resistance was reached, compared to the force controlled approach exercised in tests and in calibration procedure.

The shear resistance of each component was compared with the shear resistance of the r. c. frame without masonry infill wall (bare frame) $V_{R,f}$ (kN) at drift ratios d_r (%) 0.10, 0.25, 0.5, 0.75, 1.0, 1.25, 1.5, 1.75 and 2%. The named drift ratios correspond to the damage grades 1 to 5 based on EMS-98 damage scale [15,16]. The shear resistance ratio was expressed as V_R / $V_{R,f,max}$ × 100 (%), where $V_{R,f,max}$ is the maximal shear resistance of the r. c. frame without masonry infill wall. The shear resistance values were observed at the feet of the r. c. column, r. c. confining element or at the base of the masonry infill wall, as the sum of internal forces along the length of each individual component. In case of the eccentric opening the analysis was performed separately from left (positive) and right (negative) side.

The results are presented in Figures 6 and 7 and in Tables 7 to 9.

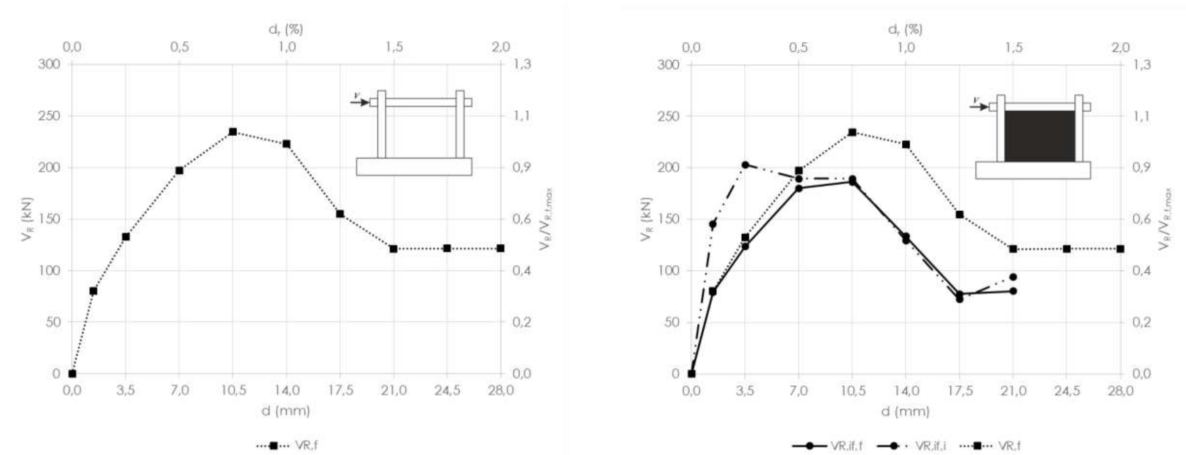

Figure 6: Shear resistance of r. c. frame without masonry infill wall (left) and of r. c. frame with masonry infill wall without openings (right) by components

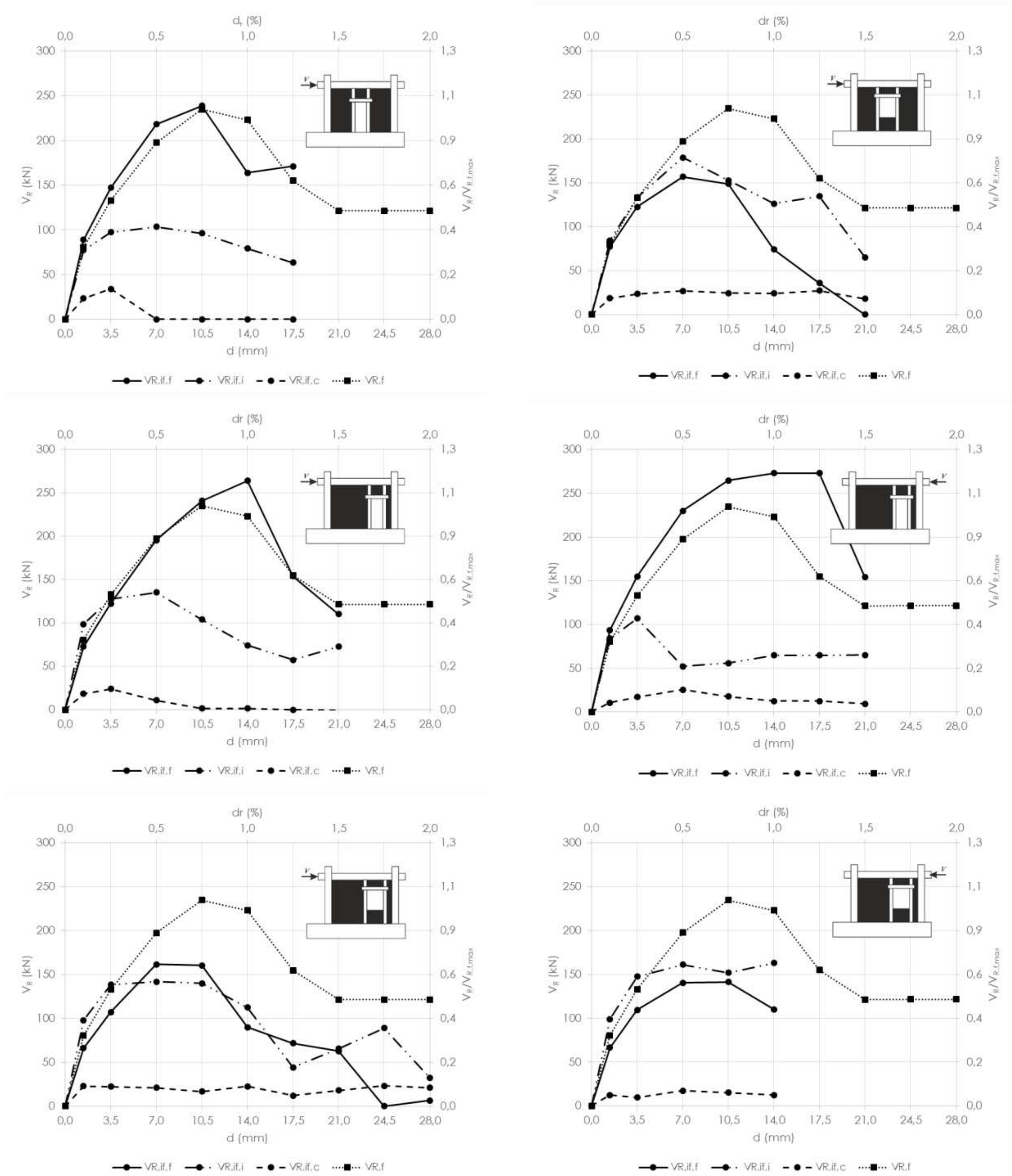

Figure 7: Shear resistance of r. c. frame with masonry infill wall, containing confined window and door openings, by components

The damage grades in compliance with the EMS-98 damage scale and corresponding drift ratio considered in this study were: Grade 1: Negligible to slight damage (no structural damage, slight non-structural damage) at d_r equal to 0.1%; Grade 2: Moderate damage (slight structural damage, moderate non-structural damage) at d_r ranges from 0.2 to 0.4%; Grade 3: Substantial to heavy damage (moderate structural damage, heavy non-structural damage) at d_r equal to 0.5%; Grade 4: Very heavy damage (heavy structural damage, very heavy non-structural damage) at d_r ranges from 0.75 to 1.0%; Grade 5: Destruction (very heavy structural damage) at d_r equal to 2.0%.

Group		**III**		**II**					
Number		**1**	**2**	**1**	**2**	**3 (P)**	**3 (N)**	**4 (P)**	**4 (N)**
d_r (%)	**d (mm)**	**$V_{R,f}$ (kN)**	**$V_{R,if,f}$ (kN)**	**$V_{R,if,f}$ (kN)**					
0.0	0.0	0	0	0	0	0	0	0	0
0.1	1.4	80	80	89	77	73	93	66	66
0.25	3.5	133	124	147	123	122	155	107	110
0.5	7.0	197	180	218	157	196	230	161	140
0.75	10.5	235	187	239	149	241	265	160	141
1.0	14.0	223	134	164	74	264	273	90	110
1.25	17.5	155	78	171	36	154	273	72	-
1.5	21.0	121	81	-	0	110	154	63	-
1.75	24.5	121	-	-	-	-	-	0	-
2.0	28.0	121	-	-	-	-	-	6	-
$V_{R,max}$ (kN)		**235**	**187**	**239**	**157**	**264**	**273**	**161**	**141**
$V_{R,max}$ / $V_{R,max,f}$ × 100 (%)		**100**	**79**	**102**	**67**	**112**	**116**	**69**	**60**

Table 7: Shear resistance contribution of r. c. frame component

Group		**III**		**II**					
Number		**1**	**2**	**1**	**2**	**3 (P)**	**3 (N)**	**4 (P)**	**4 (N)**
d_r (%)	**d (mm)**	**$V_{R,f}$ (kN)**	**$V_{R,if,I}$ (kN)**	**$V_{R,if,I}$ (kN)**					
0.0	0.0	0	0	0	0	0	0	0	0
0.1	1.4	80	146	77	84	99	84	98	99
0.25	3.5	133	203	97	133	127	107	138	148
0.5	7.0	197	190	103	179	135	52	142	161
0.75	10.5	235	189	96	153	104	56	140	152
1.0	14.0	223	130	79	126	74	65	112	163
1.25	17.5	155	72	63	135	57	65	44	-
1.5	21.0	121	94	-	65	73	65	65	-
1.75	24.5	121	-	-	-	-	-	89	-
2.0	28.0	121	-	-	-	-	-	32	-
$V_{R,max}$ (kN)		**235**	**203**	**103**	**179**	**135**	**107**	**142**	**163**
$V_{R,max}$ / $V_{R,max,f}$ × 100 (%)		**100**	**87**	**44**	**76**	**58**	**46**	**60**	**69**

Table 8: Shear resistance contribution of masonry infill wall component

Group		**III**		**II**					
Number		**1**	**2**	**1**	**2**	**3 (P)**	**3 (N)**	**4 (P)**	**4 (N)**
d_r (%)	**d (mm)**	**$V_{R,f}$ (kN)**	**$V_{R,if,c}$(kN)**	**$V_{R,if,fc}$(kN)**					
0.0	0.0	0	-	0	0	0	0	0	0
0.1	1.4	80	-	23	18	18	10	23	13
0.25	3.5	133	-	34	23	24	17	22	9
0.5	7.0	197	-	0	27	11	25	21	17
0.75	10.5	235	-	0	24	2	18	17	15
1.0	14.0	223	-	0	24	1	12	23	13
1.25	17.5	155	-	0	27	0	12	12	-
1.5	21.0	121	-	-	18	0	9	18	-
1.75	24.5	121	-	-	-	-	-	23	-
2.0	28.0	121	-	-	-	-	-	21	-
$V_{R,max}$ (kN)		**235**	**235**	**34**	**27**	**24**	**25**	**23**	**17**
$V_{R,max}$ / $V_{R,max,f}$ × 100 (%)		**100**	**100**	**15**	**12**	**10**	**11**	**10**	**7**

Table 9: Shear resistance contribution of r. c. confining element component

4 DISCUSSION OF RESULTS

Distribution of shear resistance among components of r. c. frames with masonry infill walls containing confined door and window openings, and walls without openings obtained by computations using calibrated micromodel, is given in Tables 7 to 9 and Figures 7 and 8, at selected drift ratios i.e. damage grades in compliance with EMS-98 scale. The shear resistance contribution of r. c. frame and masonry infill wall component reached its maximum at drift ratio of in either 0.75 % or 1 % in all cases (DG 4). In general, the opening type, presence and position influence the shear resistance distribution among components.

In Figure 8 given is the overall comparison of ratio of maximum shear resistance of individual component and maximum shear resistance of r. c. frame without masonry infill wall (bare frame) $V_{R,max} / V_{R,f,max} \times 100$ (%).

As observed in Figure 8, the shear resistance of the r. c. frame components was different from case to case and was influenced by opening presence. It was lower up to 40 % or equal in case of walls with window openings and wall without openings and **higher of about 12 to 16 % in the case of walls with door openings irrespective of the opening position**. It was not significantly affected by loading direction in case of walls with eccentric door or window openings, as in case without r. c. confining elements [13].

The contribution of the masonry infill wall component was influenced by opening type, presence and position. The lowest contribution of 44 and 46 % was obtained in the cases of walls with door openings. The highest contribution of 87 % was in the case of wall without openings. It was not significantly affected by loading direction in case of walls with eccentric window openings. In the case of walls with door openings the difference in contribution caused by loading direction was 12 %.

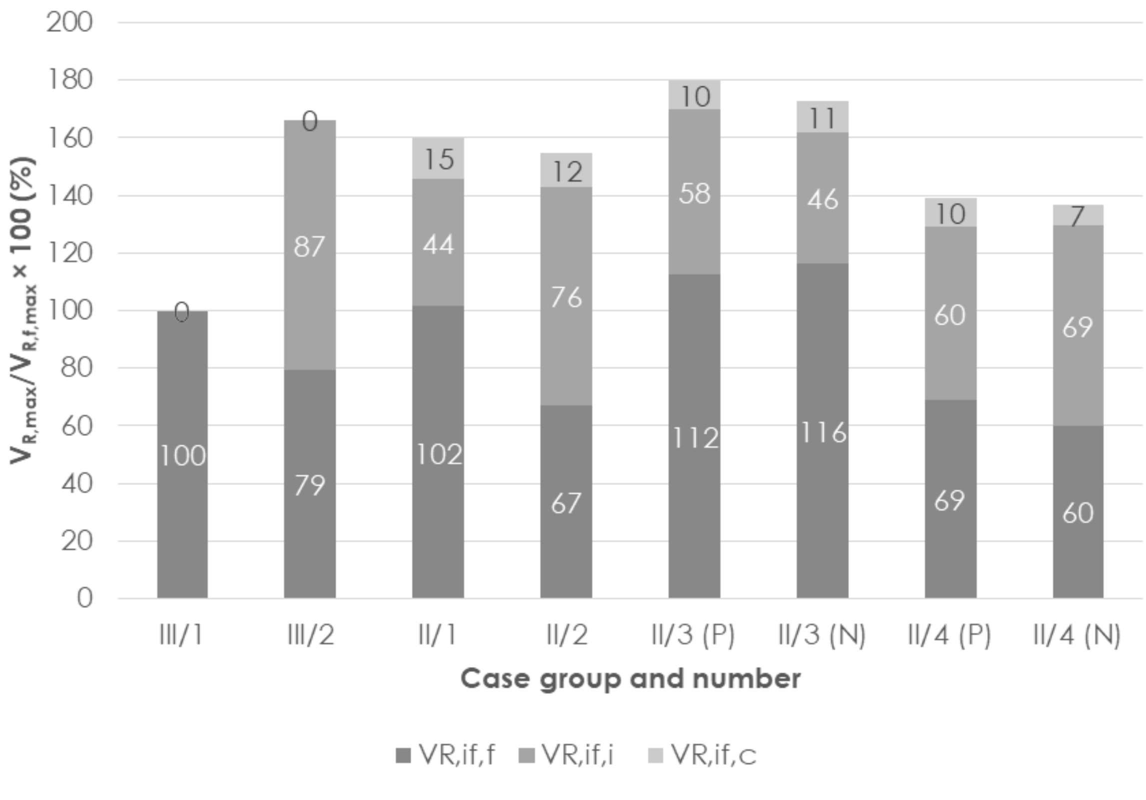

Figure 8: Shear resistance of components of r. c. frame with masonry infill wall comparison

The r. c. confining element shear resistance contribution was in average 11 %, and it was more pronounced in case of centrically positioned opening (up to 15 % in case of door and 12 % in case of window opening). As shown in Figure 7, the contribution of r. c. confining elements in case of walls with door opening, was up to drift ratio of 0.5 % (DG 2 or DG 3). On the other hand, in case of window openings, it was up to the drift ratio of the structure destruction.

As shown in Figure 7, in cases of walls with openings, after reaching the maximum shear resistance (after d_r=0.75 or 1 %), r. c. confining elements prevented the rapid drop of shear resistance of masonry infill wall component.

5 CONCLUSIONS

A calibrated computational micromodel of a tested 1/2.5 scaled r. c. frame with masonry infill wall, containing eccentrically and centrically positioned medium size confined window and door openings, and wall without openings, was used to determine the distribution of shear resistance among the structure components. The model had the ability to fully simulate tests by taking into account opening type, size and position and confining elements in a straight forward manner.

The following observations and conclusions about the distribution of shear resistance among the structure components, namely r. c. frame, masonry infill wall and r. c. confining elements, were drawn, with respect to opening type and position:

- In case of walls with window opening, and wall without opening, the shear resistance distribution among r. c. frame and masonry infill component was approximately equal, while in the case of wall with door opening, it was dominant in r. c. frame component.
- In case of walls with eccentrically positioned door openings the shear taken by the r. c. frame component was higher than in the case of r. c. frame without masonry infill wall (bare frame) i.e. design value of shear resistance capacity.
- The r. c. confining elements mitigated the influence of the loading direction in case of walls with eccentrically positioned openings and enabled for the structure to hold shear resistance to higher drift ratio values.

In general, the shear resistance distribution among the structure components was different from case to case, and was influenced by opening type and position and the presence of r. c. confining element. The construction and design of r. c. confining elements for shear resistance is fully recommended, in order to provide them with sufficient resistance up to the design drift ratio values.

REFERENCES

[1] CEN. Eurocode 2: Design of concrete structures - Part 1-1: General rules and rules for buildings (EN 1992-1-1:2004). Brussels: European Committee for Standardization; 2004.

[2] CEN. Eurocode 6: Design of masonry structures - Part 1-1: General rules for reinforced and unreinforced masonry structures (EN 1996-1-1:2005). Brussels: European Committee for Standardization; 2005.

[3] CEN. Eurocode 8: Design of Structures for Earthquake Resistance - Part 1: General Rules, Seismic Actions and Rules for Buildings (EN 1998-1:2004). Brussels: European Committee for Standardization; 2004.

[4] Penava D. Influence of openings on seismic response of masonry infilled reinforced concrete frames. PhD thesis. Josip Juraj Strossmayer University of Osijek, Osijek, Croatia; 2012.

[5] Sigmund V, Penava D. Influence of openings, with and without confinement, on cyclic response of infilled R-C frames - An experimental study. J Earthq Eng. 2014;18(1):113–46.

[6] Al-Chaar GK, Lamb GE, Issa MA. Effect of openings on structural performance of unreinforced masonry infilled frames. ACI Spec Publ. 2003;211:247–62.

[7] Decanini LD, Liberatore L, Mollaioli F. The Influence of Openings on the Seismic Behaviour of Infilled Framed Structures. In: 15th World Conference on Earthquake Engineering. Lisabon, Portugal; 2006.

[8] Kakaletsis DJ, Karayannis CG. Experimental investigation of infilled R/C frames with eccentric openings. Struct Enginering Mech J. 2007;26(231–250).

[9] Kakaletsis DJ, Karayannis CG. Influence of masonry strength and openings on infilled R/C frames under cycling loading. J Earthq Eng. 2008;12(2):197–221.

[10] Kakaletsis DJ, Karayannis CG. Experimental investigation of infilled reinforced concrete frames with openings. ACI Struct J. 2009;106(2):132–41.

[11] Tasnimi AA, Mohebkhah A. Investigation on the behaviour of brick-infilled steel frames with openings, experimental and analytical approaches. Eng Struct. 2011;33.

[12] Sigmund V, Penava D. Influence of openings, with and without confinement, on cyclic response of infilled R-C frames - An experimental study. J Earthq Eng. 2014;18(1):113–46.

[13] Penava D, Sarhosis V, Kožar I, Guljaš I. Contribution of RC columns and masonry wall to the shear resistance of masonry infilled RC frames containing different in size window and door openings. Eng Struct. 2018 Oct;172:105–30.

[14] Sigmund V, Penava D. Assessment of masonry infilled reinforced concrete frames with openings. Tech Gaz. 2013 Jun 15;20(3):459–66.

[15] Grünthal G, Musson RMW, Schwarz J, Stucchi M. European macroseismic scale 1998. Centre Européen de Géodynamique et de Séismologie. Luxembourg; 1998.

[16] Schwarz J, Abrahamczyk L, Leipold M, Wenk T. Vulnerability assessment and damage description for R.C. frame structures following the EMS-98 principles. Bull Earthq Eng. 2015;13(4):1141–59.

[17] Cervenka V, Jendele L, Cervenka J. ATENA Program Documentation Part 1 Theory. Prague: Cervenka Consulting Ltd.; 2012.

[18] Pryl D, Cervenka J. ATENA program documentation, part 1 of 1, troubleshooting manual. Prague: Cervenka Consulting Ltd.; 2013.

[19] Cervenka Consulting s.r.o. ATENA for Non-Linear Finite Element Analysis of Reinforced Concrete Structures. Prague: Červenka Consulting s.r.o.; 2015.

[20] Penava D, Sigmund V, Kožar I. Validation of a simplified micromodel for analysis of infilled RC frames exposed to cyclic lateral loads. Bull Earthq Eng. 2016;14(10):1–26.

[21] Asteris PG, Cavaleri L, Di Trapani F, Tsaris AK. Numerical modelling of out-of-plane response of infilled frames: State of the art and future challenges for the equivalent strut macromodels. Vol. 132, Eng Struct. 2017.

[22] Asteris PG, Cavaleri L, Di Trapani F, Sarhosis V. A macro-modelling approach for the analysis of infilled frame structures considering the effects of openings and vertical loads. Struct Infrastruct Eng. 2016 May 3;12(5):551–66.

[23] Crisafulli FJ, Carr AJ, Park R. Analytical modelling of infilled frame structures - a general review. Bull New Zeal Soc Earthq Eng. 2000;33(1):30–47.

[24] Di Trapani F, Bertagnoli G, Ferrotto MF, Gino D. Empirical Equations for the Direct Definition of Stress–Strain Laws for Fiber-Section-Based Macromodeling of Infilled Frames. J Eng Mech. 2018

[25] Cavaleri L, Di Trapani F. Prediction of the additional shear action on frame members due to infills. Bull Earthq Eng. 2015 May 2;13(5):1425–54.

[26] Furtado A, Rodrigues H, Arêde A. Modelling of masonry infill walls participation in the seismic behaviour of RC buildings using OpenSees. Int J Adv Struct Eng. 2015;7(2).

[27] Laughery L, Pujol S. Compressive strength of unreinforced struts. ACI Struct J. 2015;112(5).

[28] Asteris PG, Cotsovos DM, Chrysostomou CZ, Mohebkhah A, Al-Chaar GK. Mathematical micromodeling of infilled frames: state of the art. Eng Struct. 2013;56:1905–21.

[29] Campbell J. Numerical Model for Nonlinear Analysis of Masonry Walls. PhD Thesis. Rheinisch –Westfälische Technische Hochschule Aachen; 2012.

[30] Al-Chaar GK, Mehrabi, A. Constitutive models for nonlinear finite element analysis of masonry prisms and infill walls. ERDC/CERL TR- 08-19. Construction Engineering Research Laboratory US Army Corps of Engineers. Engineer Research and Development Centre. Washington, DC; 2008.

[31] Koutromanos I. Numerical Analysis of Masonry-Infilled Reinforced Concrete Frames Subjected to Seismic Loads and Experimental Evaluation of Retrofit Techniques. PhD Thesis. University of California, San Diego; 2011.

[32] Sarhosis V, Tsavdaridis KD, Giannopoulos I. Discrete Element Modelling of Masonry Infilled Steel Frames with Multiple Window Openings Subjected to Lateral Load Variations. Open Constr Build Technol J. 2014;8(1):93–103.

[33] Mohebkhah A, Tasnimi AA, Moghadam HA. Nonlinear analysis of masonry-infilled steel frames with openings using discrete element method. J Constr Steel Res. 2008 Dec [cited 2017 Jul 28];64(12):1463–72.

[34] Penava D, Sigmund V, Kožar I, Anić F, Trajber D, Vig M. Clay block masonry and mortar joint interlocking. J Croat Assoc Civ Eng. 2016 Sep;68(08):609–16.